

## States in $^{14}\text{C}$ from $\sigma_T$ and $\sigma_{el}(\theta)$ for $^{13}\text{C}+n$ : Measurement, $R$ -matrix analysis, and model calculations

R. O. Lane, H. D. Knox, and P. Hoffmann-Pinther

*John E. Edwards Accelerator Laboratory, Ohio University, Athens, Ohio 45701*

R. M. White

*University of California, Lawrence Livermore National Laboratory, Livermore, California 94550*

G. F. Auchampaugh

*University of California, Los Alamos National Scientific Laboratory, Los Alamos, New Mexico 87545*

(Received 16 October 1980)

Differential elastic scattering cross sections for neutrons scattered from  $^{13}\text{C}$  have been measured at 9 angles from  $20^\circ$  to  $160^\circ$  for  $1.25 \text{ MeV} \leq E_n \leq 6.5 \text{ MeV}$ . These data together with high-resolution total cross section measurements were analyzed by means of a multichannel-multilevel  $R$ -matrix program to determine  $J$ ,  $\pi$ ,  $\gamma_{\lambda c}$ , and other parameters of many newly assigned states up to  $E_x = 14 \text{ MeV}$  in  $^{14}\text{C}$ . This extensive and in-depth investigation of  $^{14}\text{C}$  provided a basis for comparison to nuclear model predictions over a wide range of excitation energy. A core-coupling model was employed to calculate states in  $^{14}\text{C}$  as well as nucleon spectroscopic factors for reactions leading to these states. Calculations of states in  $^{14}\text{C}$  via both effective interactions and a weak coupling model, together with those from the core-coupling model, were compared to results of the  $R$ -matrix analysis. Much of the structure observed in the experimental work is predicted by the models.

[
 NUCLEAR REACTIONS  $^{13}\text{C}(n,n)^{13}\text{C}$ ,  $1.25 \leq E_n \leq 6.5 \text{ MeV}$ , measured  $\sigma(\theta)$ ,  $R$ -matrix analysis,  $^{14}\text{C}$  deduced  $J^\pi$ ,  $\gamma_{\lambda c}$ .  
 NUCLEAR STRUCTURE  $^{14}\text{C}$ , calculated negative parity states, core coupling.  
 Comparison to other models.

### I. INTRODUCTION

Above an excitation energy of  $E_x = 9 \text{ MeV}$  in  $^{14}\text{C}$ , the relatively few experimental investigations<sup>1-6</sup> of this nucleus have given a number of either conflicting or tentative assignments for  $J$ ,  $\pi$ , and other properties of states. Only a very few assignments appear to be firm.<sup>6</sup> None of the firm assignments were made in this region by neutron interactions with  $^{13}\text{C}$ . Moreover, no differential neutron cross section measurements had been reported for  $^{13}\text{C}$ . The recent high resolution total neutron cross section data of Auchampaugh *et al.*<sup>7</sup> up to a neutron energy of  $E_n = 14 \text{ MeV}$  ( $E_x \approx 21 \text{ MeV}$ ) showed in great detail considerable resonance structure whose analysis might well lead to a substantial improvement in our knowledge of the  $^{14}\text{C}$  system. It was decided that differential neutron elastic scattering cross sections  $\sigma_{el}(\theta)$  measured over the broader resonances together with the high resolution total cross sections<sup>7</sup> on narrow resonances at lower energies should, especially when analyzed together, be very helpful in determining neutron properties and  $J^\pi$  of states in  $^{14}\text{C}$ . By the comparison of these results to model calculations, the predicted theoretical states, configurations, and nucleon spectroscopic factors

can then be tested. The following section gives a brief description of the experimental method which was described in detail earlier.<sup>8</sup> Since the  $R$ -matrix analysis program for elastic scattering employed in this work was also described previously,<sup>8</sup> only those comments of particular relevance to the  $^{13}\text{C}$  scattering problem will be given in the section on  $R$ -matrix fitting. Finally, in the last section recent core-coupling model calculations made by the authors and shell model calculations by others will be described and their predictions will be compared to the experimental results.

### II. EXPERIMENTAL PROCEDURE AND RESULTS

A complete development of the experimental method is given in Ref. 8 and references contained therein. The Ohio University tandem Van de Graaff accelerator produced a proton beam of  $4 \mu\text{A}$  average current pulsed and bunched to  $\sim 0.75 \text{ ns}$  full width at half maximum (FWHM) at a repetition rate of  $5 \text{ MHz}$ . The beam was incident on a tritium gas cell which produced neutrons with an FWHM energy spread of  $\sim 60 \text{ keV}$  in the forward direction via the reaction  $^3\text{H}(p,n)^3\text{He}$ . The neutrons were then scattered from a sample of  $40.75$

g of  $^{13}\text{C}$  powder pressed into a thin aluminum can. The sample was enriched to 98% in  $^{13}\text{C}$ . The neutron detector was an NE 213 liquid scintillator 5 cm thick by 11.25 cm diameter optically coupled to an RCA 4522 photomultiplier tube. The system provided very effective discrimination against  $\gamma$  rays. The flight path from the scatterer to detector was 3.6 m. The detector shielding, the flux monitoring, cross section determination, multiple scattering corrections, error calculations, and other experimental details are available in Ref. 8.

Differential cross section measurements were made at nine equally spaced angles from  $20^\circ$  to  $160^\circ$  inclusive at each energy. The bias for neutron detection was set at 450 keV. As in earlier work from this laboratory frequent measurements of the differential elastic scattering cross section for  $^{12}\text{C}$  were made at several energies interspersed among the  $^{13}\text{C}$  measurements. In all cases, the well-known  $^{12}\text{C}$  data were reproduced to good accuracy. Thus these independent checks over a substantial period of time provided an overall confirmation of the accuracy of the cross sections.

The measured differential elastic scattering cross sections from the present experiment are shown as data points in Fig. 1 in the form of Legendre polynomial coefficients  $B_L$ . Expansions including terms of  $L \geq 5$  gave higher order coefficients that were statistically zero, so that expansions for  $L \leq 4$  were adequate.

### III. R-MATRIX ANALYSIS AND DISCUSSION

The interaction radius  $a$  was chosen to be 4.5 fm based in part on earlier  $R$ -matrix fitting for neutron scattering from a neighboring nucleus  $^{11}\text{B}$ . Values for the constant terms  $R_c^{j^*}$  were determined by fitting the average values of the  $B_L$ . The boundary conditions  $b_c$  were chosen to produce zero shift in the resonance energies near the middle of the energy range studied. Figure 2 shows the level structure of  $^{14}\text{C}$  as determined from the present work together with well-established states from other experiments. The solid curves of Figs. 1 and 3-6 are the results of the final  $R$ -matrix calculation for elastic scattering and the parameters for these are given in Table I.

In order to make a more valuable contribution and coordinate the available data for  $^{13}\text{C} + n$  as well as pertinent charged-particle work on  $^{14}\text{C}$ , the results of an  $R$ -matrix analysis of the  $\sigma_T$  data of Auchampaugh *et al.*<sup>7</sup> up to  $E_n \approx 3$  MeV will be discussed first together with comparisons to earlier work. Then the  $R$ -matrix analysis of the present data for  $E_n \geq 3$  MeV will be discussed.

#### A. Bound states and low-energy total cross sections

The high-resolution total cross section data of Ref. 7 obtained for a high enrichment (90%) sample of  $^{13}\text{C}$  are shown from  $1.25 \leq E_n \leq 8$  MeV in Fig. 3. Below the first inelastic threshold of  $E_n \sim 3.3$  MeV there are no other particle channels open and  $\sigma_T = \sigma_{el}$ . The  $R$ -matrix program ORMAP, which calculates elastic scattering cross sections, was used to extract resonance parameters from these total cross section data. In this energy region the  $^{13}\text{C}(n, \gamma)^{14}\text{C}$  cross section is negligible.

Earlier measurements of  $\sigma_T$  by Cohn *et al.*<sup>1</sup> exist for energies of  $0.1 \leq E_n \leq 9$  MeV. However, these data were obtained with relatively large energy spreads and a transmission sample of low enrichment in  $^{13}\text{C}$  (58.3%). Furthermore, the data have rather large errors which is apparent in the substantial fluctuations from point to point in regions of smooth cross section. When compared to the data of Ref. 7 and the integrated elastic scattering data from the present results up to  $E_n \sim 3.5$  MeV, the results of Cohn *et al.*<sup>1</sup> are clearly and consistently high by  $\sim 10$ – $15\%$ . Below 1.25 MeV no other extensive measurements of  $\sigma_T$  have been reported. Therefore, the average off-resonance values of the data of Cohn *et al.*<sup>1</sup> below this energy were normalized downward by 10–15% at all  $E_n < 1.25$  MeV and were taken as the guide to the fitting of the cross section at low energies. The effects of the large  $s$ -wave contributions by the strong bound  $1^-$  state at  $E_x = 6.09$  MeV, and the equally strong  $0^-$  bound state at  $E_x = 6.90$  MeV are obvious in the rapid rise in  $\sigma_T$  with decreasing energy below  $E_n \approx 2$  MeV. Because of the substantial effect these states have on the nonresonant background for the  $R$ -matrix fitting at virtually all neutron energies considered here, an effort was made to represent as well as possible the contributions of these bound states to the total cross section. The most recent determination of  $\theta^2$  for these states by the reaction  $^{13}\text{C}(d, p)^{14}\text{C}$  is that of Glover and Jones<sup>9</sup> who obtained a value of  $\theta^2 \approx 0.2$  for both the  $1^-$  state at  $E_x = 6.09$  MeV and the  $0^-$  state at  $E_x = 6.90$  MeV. The interaction radius (4.5 fm) for the present  $R$ -matrix analysis was chosen on the basis of previous studies including  $^{11}\text{B}(n, n)^{11}\text{B}$ . Quite coincidentally Glover and Jones also used the same radius in their stripping analysis. So, perhaps it is not surprising that the values of  $\theta^2 \approx 0.15$  [where  $\theta^2 = \gamma^2 / (3\hbar^2 / 2\mu a^2)$ ] for the present work agree well with those of Glover and Jones. The parameters for these bound states are shown in Table I. The  $E_\lambda$  include the effects of  $s$ -wave shifts for negative energy channels. The relatively narrow resonance at  $E_n = 0.15$  MeV ( $E_x = 8.32$  MeV) has been assigned  $2^+$  from

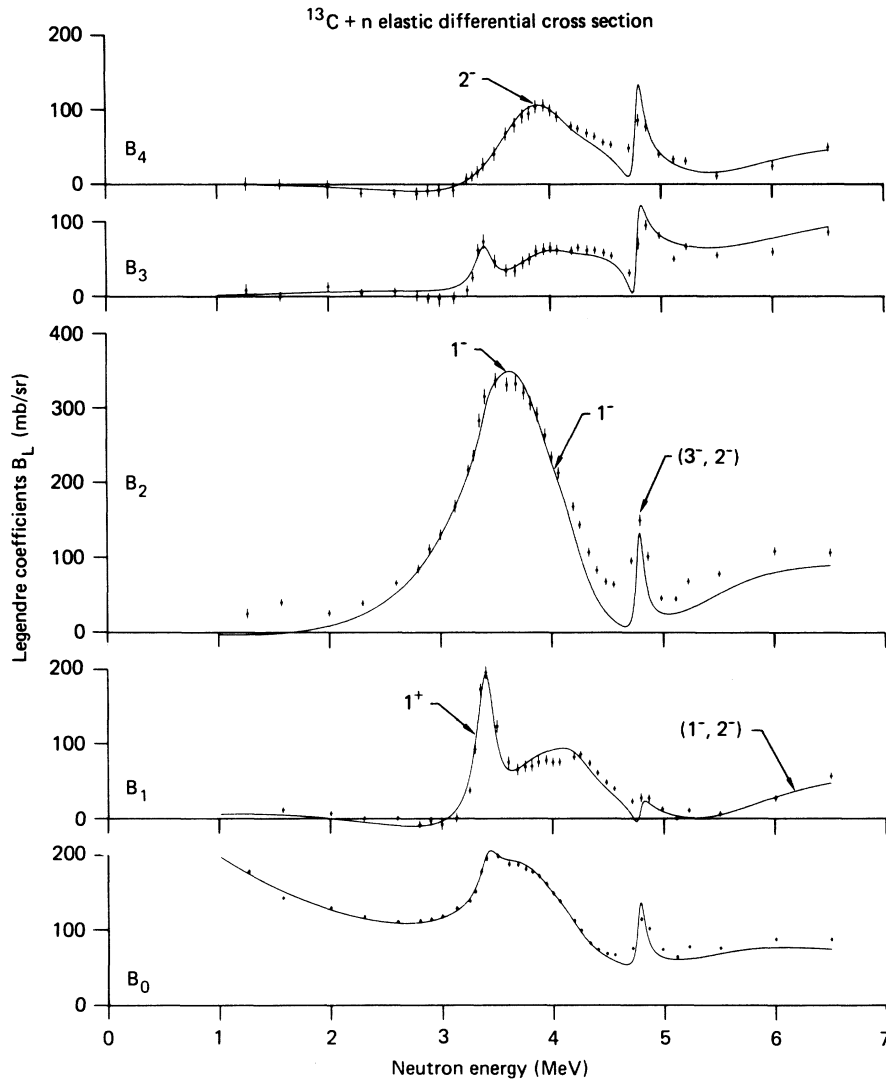


FIG. 1. Coefficients  $B_L$  in the Legendre polynomial expansion of the differential elastic cross section  $\sigma_{e1}(\theta) = \sum B_L P_L(\cos \theta)$  for  $L=0$  to 4 for the measurements of neutrons scattered from  $^{13}\text{C}$ . Coefficients are in the c.m.s. while energies are in the laboratory system. The curves are the results of the  $R$ -matrix fit to all the data, and are based on parameters of Table I. The  $J^\pi$  assignments to broad states from this analysis above a neutron energy of 3 MeV are indicated by arrows.

several other investigations<sup>6</sup> and was not included in these studies.

B. Narrow resonances,  $1.25 \leq E_n \leq 3.5$  MeV,  
from  $\sigma_T$  data

From the reaction  $^{12}\text{C}(t,p)^{14}\text{C}$ , Mordechai *et al.*<sup>5</sup> observe a clear  $0^+$  state in  $^{14}\text{C}$  at  $E_x = 9.746$  MeV which would correspond to  $E_n = 1.69$  MeV. Figure 4 shows in more detail the cross section in this region, and there is no indication of any neutron resonance near this energy. This is not at all surprising since such a state is expected<sup>10</sup> to be predominantly two neutrons in the  $sd$  shell cou-

pled to a  $^{12}\text{C}$  core, which is much more likely to be observed in the reaction  $^{12}\text{C}(t,p)^{14}\text{C}$  than in  $^{13}\text{C}(n,n)^{13}\text{C}$ .

Near  $E_n = 1.75$  MeV ( $E_x = 9.8$  MeV) there is an anomaly which in previous work<sup>1,3,5</sup> has been observed with poorer energy resolution and was treated as a single level with the result that it has been given conflicting assignments. However, from the recent high resolution work of Ref. 7, it is clearly seen in Figs. 3 and 4 that the anomaly is, in fact, composed of a narrow resonance peak ( $E_n = 1.736$  MeV) superimposed almost directly over a broader  $s$ -wave dip ( $E_n = 1.754$  MeV). Extensive parameter searches for best fits were

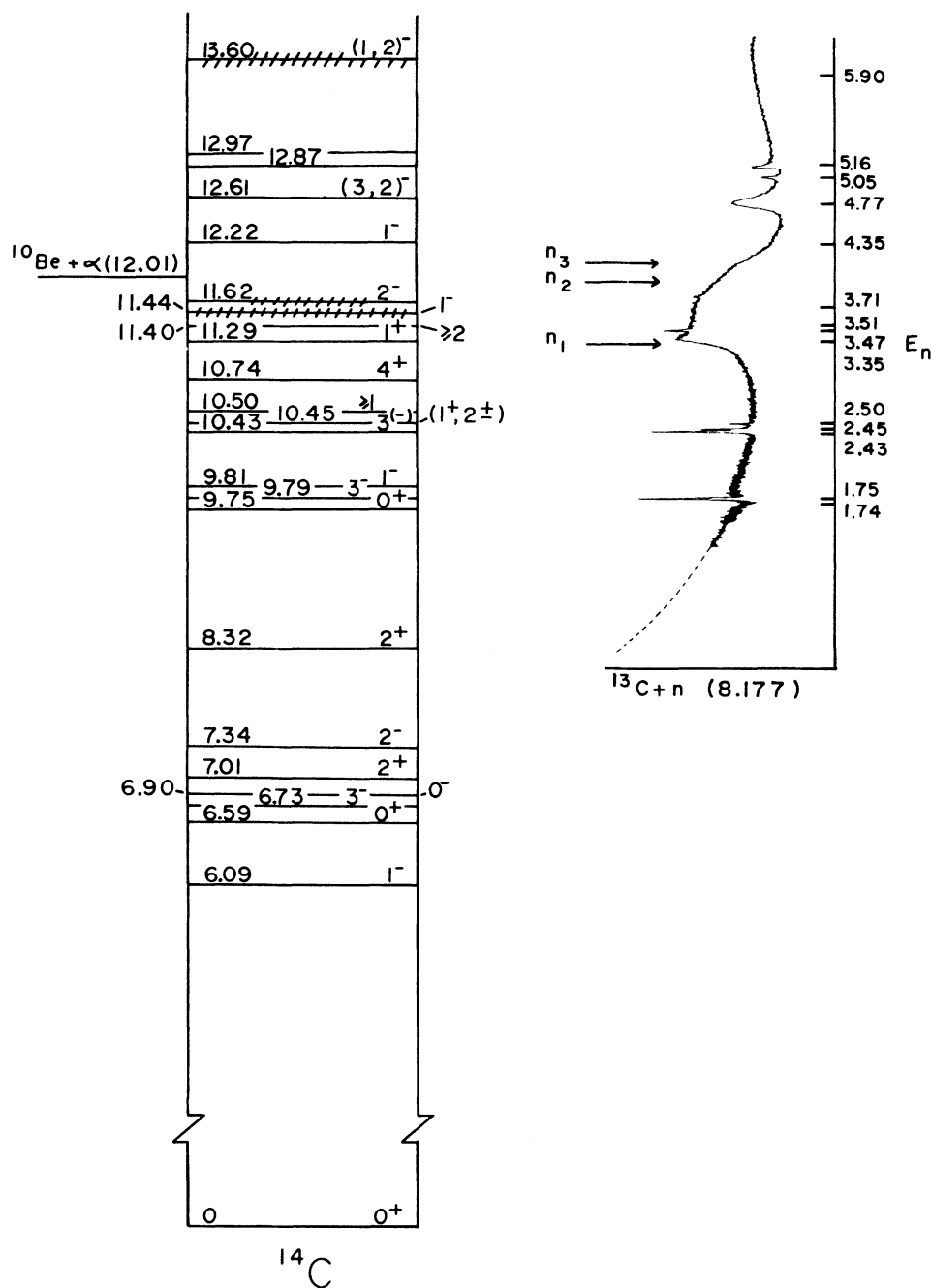


FIG. 2. Energy level diagram for  $^{14}\text{C}$ . The  $J^\pi$  and energies include those from the present work as well as some from Refs. 5 and 6. Energies have been rounded to two decimal places for clarity of presentation. The total cross section data of Ref. 7 are plotted on the right as a function of neutron energy to aid in the identification of states. The dashed curve represents the  $R$ -matrix fit to the average nonresonant renormalized data of Ref. 1 at low energies (see text). Thresholds for the inelastic processes  $^{13}\text{C}(n, n')^{13}\text{C}^*$  (3.09, 3.68, and 3.85 MeV) are shown as arrows labeled  $n_1$ ,  $n_2$ , and  $n_3$ .

carried out for various possible pairs of assignments for these two states. Only the two combinations of  $3^-(\text{peak})-1^-(\text{dip})$  and  $3^-(\text{peak})-1^-(\text{dip})$  gave accurate fits to the detailed features of these res-

onances. The experimental energy spread ( $\approx 3.5$  keV FWHM) at this energy had very little averaging effect on these resonances; nevertheless a Gaussian resolution function of FWHM = 3.5 keV

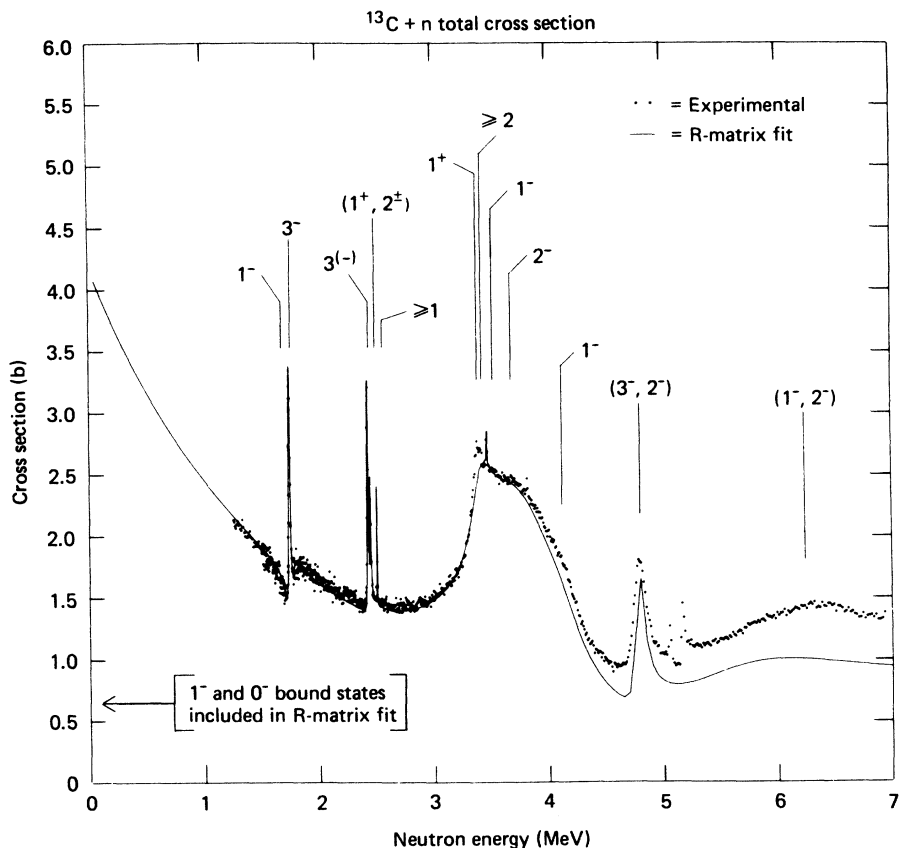


FIG. 3. Total cross section  $\sigma_T$  (points) from Ref. 7 and integrated elastic scattering cross section  $\sigma_{e1}$  (curve) from  $R$ -matrix analysis for  $^{13}\text{C}+n$ . The  $J^\pi$  assignments and approximate locations for states in  $^{14}\text{C}$  resulting from the  $R$ -matrix analysis are indicated in the figure. Only a representative number from the full set of data points for  $\sigma_T$  are shown to portray adequately the features of the total cross section. The scatter in the points is taken as the measure of errors on  $\sigma_T$ . For the  $1^-$  resonance near 1.75 MeV the location of the resonance dip is indicated rather than the calculated resonance energy (see Fig. 4).

was used to give the curve shown in Fig. 4. The fits for  $3^+-1^-$  and  $3^--1^-$  were essentially identical, but the  $3^+$  would require  $f$ -wave neutrons with a  $\gamma^2$  of 0.8 MeV which is most unlikely at this energy. Therefore, the narrow resonance is assigned  $3^-$ . The fit for the  $3^-$  assignment is shown in Fig. 4. There is little, if any, doubt concerning the  $1^-$  assignment for the dip. These two states at  $E_x = 9.789$  and  $9.806$  MeV are assigned  $3^-$  and  $1^-$ , respectively.

Near  $E_n \approx 2.4$  MeV of Fig. 3 there exists sharp resonance structure in  $\sigma_T$ . Figure 5 shows an expanded view of this region revealing three resolved resonances. The fit has been averaged with a Gaussian of FWHM = 5.7 keV corresponding to the resolution of Ref. 7.

From previous neutron total cross section measurements, Cohn *et al.*<sup>1</sup> assigned the resonances at  $E_n = 2.43$  MeV ( $E_x = 10.429$  MeV) and 2.45 MeV ( $E_x = 10.447$  MeV), as  $J = 2$  and  $J \geq 1$ , respectively. They did not observe the small resonance at 2.5

MeV.

A calculation of  $\sigma_T$  for an assignment of  $J = 2$  to the state at  $E_n = 2.43$  MeV was made in the present  $R$ -matrix analysis and is shown as the dashed curve in Fig. 5. This assignment gives a peak height well below the data. Thus  $J \leq 2$  for this state must be excluded. The value  $J = 4$  was also excluded because the averaged cross section was much too high on the peak. Only  $J = 3$  agrees with the data. For this resonance  $3^-$  gave a better fit to the shape of the resonance, especially on the high energy side, than did the fit for  $3^+$ . A preferred assignment of  $3^-$  based on such an argument is somewhat dependent on the magnitude, phase, parity, etc., for the background and nonresonant cross sections for that  $J^\pi$ . Thus this state is assigned  $J = 3$  with the parity being most probably negative. The calculated solid curve in Fig. 5 is for  $J^\pi = 3^-$ .

For the 10.447 MeV state ( $E_n = 2.45$  MeV) the assignment of  $J^\pi = 1^+$  gave the best fit to the reso-

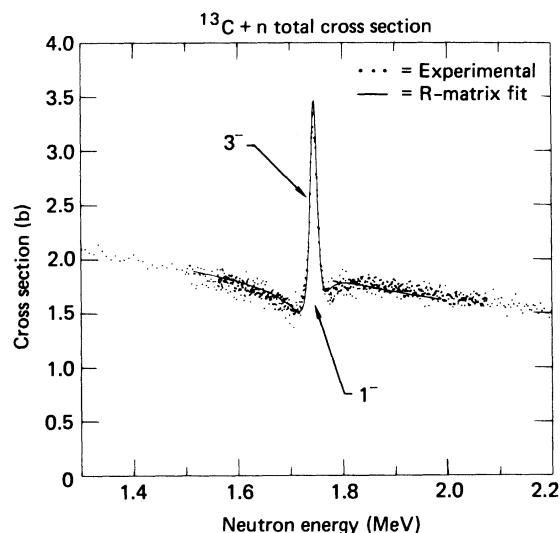


FIG. 4. Expanded plot of the total cross section (points) from Ref. 7 and integrated elastic scattering cross section (curve) from *R*-matrix analysis for  $^{13}\text{C}+n$  for the resonances near 1.75 MeV. The curve has been averaged over the experimental resolution of FWHM = 3.5 keV. Note that in Table I the energy of the  $3^-$  resonance (peak) is actually slightly lower than that of the  $1^-$  resonance (dip). The apparent reversal of this order occurs in this case because of the slight asymmetry of the  $1^-$  dip and the nearly equal energies of the resonances. The full data set for  $\sigma_T$  is shown from  $E_n \approx 1.6$  to 2.0 MeV while only a partial set is displayed outside this region to aid in relating to other figures. The scatter in the points is taken as a measure of the errors.

nance although  $J^\pi = 2^+$  could not be excluded. The preferred  $1^+$  calculation is shown in Fig. 5. This is not inconsistent with Cohn *et al.*<sup>1</sup> who gave  $J \geq 1$  for this state.

Charged particle work to date<sup>2,3,5</sup> has not resolved these two states at  $E_x = 10.429$  and 10.447 MeV. From the  $^9\text{Be}(^6\text{Li}, p)^{14}\text{C}$  reaction, Ajzenberg-Selove *et al.*<sup>3</sup> were unable to make direct assignments, but rather through indirect arguments suggested the values of  $2^+$  or  $3$  for each state. Kaschl *et al.*,<sup>2</sup> using the reaction  $^{15}\text{N}(d, ^3\text{He})^{14}\text{C}$ , did not make definite assignments either, but implied  $J^\pi = 1^+$  or  $2^+$  for one of the states. Mordechai *et al.*<sup>5</sup> from the measurements of the  $^{12}\text{C}(t, p)^{14}\text{C}$  reaction assign  $2^+$  to the lower energy state from distorted wave calculations even though they do not resolve the two states. Those authors make no statement regarding the  $J^\pi$  of the higher energy state. This  $2^+$  assignment clearly disagrees with the present results as discussed above. From the very good agreement of excitation energies between Mordechai *et al.*<sup>5</sup> and the present work it would appear that the same states are in fact being

compared. From the data of Auchampaugh *et al.*,<sup>7</sup> together with the present analysis, the assignment for the state at  $E_x = 10.429$  MeV is  $J^\pi = 3^{(-)}$ , and that for the state at 10.447 MeV is  $J^\pi = 1^+$  or  $2^+$ .

The resonance at  $E_n = 2.504$  MeV ( $E_x = 10.502$  MeV) in Fig. 5 has essentially the resolution width of the experiment, i.e.,  $\sim 5.7$  keV. From the present fitting only  $J = 0$  could be excluded, thus  $J \geq 1$  and  $\Gamma \ll 5$  for this resonance. In the reaction  $^9\text{Be}(^6\text{Li}, p)^{14}\text{C}$ , Ajzenberg-Selove *et al.*<sup>3</sup> observed a state at 10.512 MeV and assigned it  $J = 4$ , and Mordechai *et al.*<sup>5</sup> observed a state at 10.498 MeV and assigned it  $J^\pi = (3^+)$ , neither of which is inconsistent with the present work.

At  $E_x = 10.736$  MeV ( $E_n = 2.756$  MeV) a  $4^+$  state is observed<sup>5</sup> in the two-particle transfer reaction  $^{12}\text{C}(t, p)^{14}\text{C}$  and is predominantly  $(d_{5/2})^2$  coupled to the  $^{12}\text{C}$  core. A state at 10.743 MeV is also observed<sup>3</sup> in the reaction  $^9\text{Be}(^6\text{Li}, p)^{14}\text{C}$ . From the predominant configuration of that state it is not likely to be observed with much width in the neutron channel. There is possibly a slight indication of a resonance in  $\sigma_T$  at  $E_n = 2.75$  MeV (not clearly visible in Fig. 3); therefore, the neutron width of this resonance is extremely small.

At  $E_n = 3.466$  MeV ( $E_x = 11.395$  MeV) atop the very broad structure at 3.0 to 4.5 MeV in Fig. 3 is a very narrow resonance of measured width approximately 12 keV. The assignments of  $J \leq 1$  clearly disagreed with the data. In the  $^{12}\text{C}(t, p)^{14}\text{C}$  reaction Mordechai *et al.*<sup>5</sup> observe a state at  $E_x = 11.40$  MeV and make a strong claim that it is  $1^-$ . Because of the unqualified nature of the  $1^-$  assignment given by those authors to this state, a thorough search over many parameter variations of  $\gamma_{s_{1/2}}$ ,  $\gamma_{d_{3/2}}$ , and their signs was made to investigate the disagreement. No combination of parameters for  $1^-$  came even close to fitting the data. In fact this was one of the strongest cases of rejection of a  $J^\pi$  possibility in this entire work. The  $1^-$  assignment typically gave a pronounced interference dip rather than a peak as shown in Fig. 6. Variations of parameters for this resonance changed the asymmetry of this dip, but in no case was a peak produced. That an interference dip should occur in this case is readily understandable as the result of dramatic interference with the very broad  $1^-$  state at nearly the same energy in the broad structure under this narrow resonance. It is very unlikely that Mordechai *et al.*<sup>5</sup> would observe the very broad underlying  $1^-$  state since its reduced neutron width is  $\sim 0.8$  MeV. This resonance was not observed in the earlier neutron work.<sup>1</sup> A state was observed in the  $^9\text{Be}(^6\text{Li}, p)^{14}\text{C}$  reaction<sup>3</sup> also at  $E_x = 11.40$  MeV and was assigned  $2^+$  or  $3$ . The conclusion of this analysis is that  $J \geq 2$  for the resonance at  $E_n = 3.466$  MeV, which

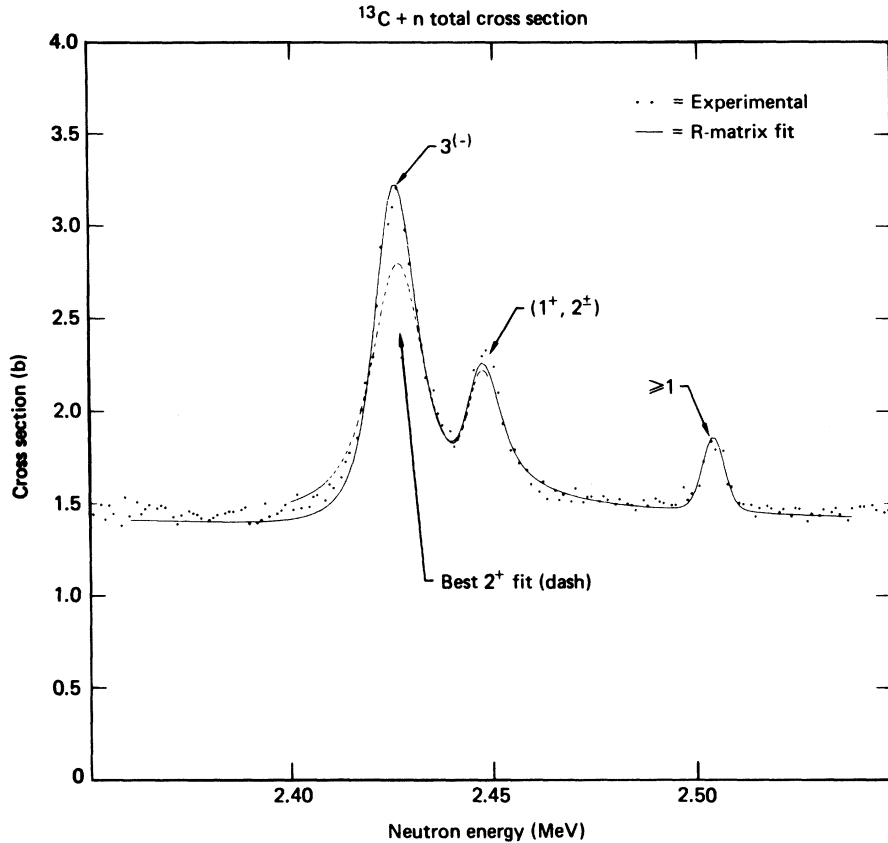


FIG. 5. Expanded plot of the total cross section (points) from Ref. 7 and integrated elastic scattering cross section (curves) from  $R$ -matrix analysis for  $^{13}\text{C}+n$  for resonances near 2.4 MeV. The curves have been averaged over the experimental resolution of FWHM=5.7 keV. The solid curve is based on the parameters of Table I for the assignments shown above the curve. The dashed curve represents the best  $R$ -matrix fit for a  $2^+$  assignment to the resonance at  $E_n=2.426$  MeV which is assigned  $3^{(-)}$  in this work. The scatter in the points is taken as a measure of the errors.

clearly disagrees with the work of Mordechai *et al.* but is consistent with the work of Ajzenberg-Selove *et al.*<sup>3</sup>

#### C. Resonances for $3 \text{ MeV} \leq E_n \leq 6.5 \text{ MeV}$ from $\sigma_{e1}(\theta)$ data

The version of ORMAP used here included only elastic scattering, which is a very good approximation up to  $E_n \sim 4.5$  MeV. Evidence that the cross sections for the first and second inelastic groups,  $n_1$  ( $E_{th}=3.326$  MeV) and  $n_2$  ( $E_{th}=3.968$  MeV), are small relative to the elastic group  $n_0$ , is apparent from the comparison of the  $R$ -matrix curve for the integrated elastic cross section  $\sigma_{e1}$  to the total cross section  $\sigma_T$  in Fig. 3. Further independent evidence on the small size of the inelastic cross sections was provided by direct measurement.<sup>11</sup>

At  $E_n=3.4$  MeV ( $E_x=11.3$  MeV) is a state characterized in Fig. 1 by a very pronounced peak in  $B_1$  and lesser ones in  $B_0$  and  $B_3$ . This clearly signals the parity as being positive. It is very prob-

able that  $l_n=1$ , since  $B_L$  for  $L > 4$  were not required to fit the data, and, furthermore, it is unlikely that at this energy a resonance with  $l_n=3$  would have such a large width. Of the possible  $J^\pi$  values, only the  $1^+$  assignment gave good agreement with the data and the  $R$ -matrix fit for this assignment is shown in Fig. 1. Extensive variations of  $\gamma_{p_{1/2}}$  and  $\gamma_{p_{3/2}}$  were tried and the values of 0.196 and 0.240, respectively, shown in Table I gave the best fit to the data. The ratio  $\gamma_{p_{3/2}}^2/\gamma_{p_{1/2}}^2$  is equal to 1.5, and values of this ratio less than 1.0 or greater than 2.0 gave fits to the resonance that were clearly outside experimental errors. Mordechai *et al.*<sup>5</sup> do not observe a state at this energy in the  $^{12}\text{C}(t,p)^{14}\text{C}$  reaction. Ajzenberg-Selove *et al.*<sup>3</sup> observe a state at  $E_x=11.306$  MeV and assign it as  $J^\pi=1^-$ , although in a later compilation<sup>6</sup> it is given as  $1^{(-)}$ . From measurements of the proton pickup reaction  $^{15}\text{N}(d,^3\text{He})^{14}\text{C}$ , Kaschl *et al.*<sup>2</sup> observed a  $1^+$  state in  $^{14}\text{C}$  at  $E_x=11.29$  MeV with a width of  $\sim 150$  keV, nearly all attributed to neutron

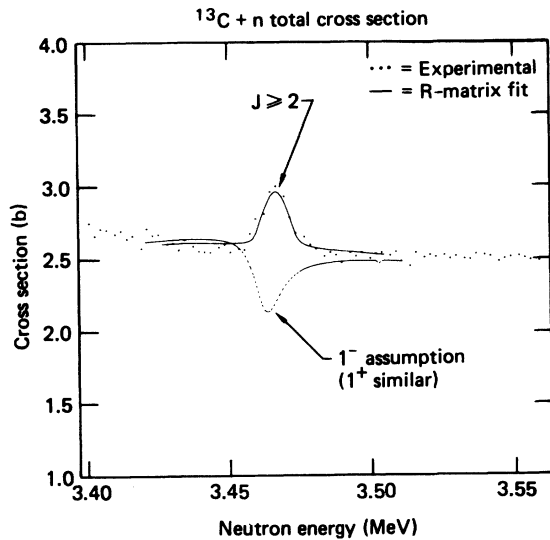


FIG. 6. Expanded plot of the total cross section (points) from Ref. 7 and the integrated elastic scattering cross section (curve) from  $R$ -matrix analysis for  $^{13}\text{C}+n$  for the resonance at  $E_n=3.466$  MeV. The solid curve is based on the  $R$ -matrix calculation for  $J \geq 2$  and averaged over a Gaussian function of FWHM = 9.6 keV. The dashed curve is for  $J^f=1^-$ . Similar results were produced for  $J^f=1^+$ . The scatter in the points is taken as a measure of the errors. (Note the suppressed zero.)

decay. This is in excellent agreement with the properties of the  $1^+$  state observed in the present experiment. Crannell *et al.*<sup>4</sup> observed from inelastic electron scattering that most of the strength of the  $M1$  transition for  $^{14}\text{C}(e, e')^{14}\text{C}$  was concentrated in a state at  $E_x=11.31$  MeV. This led to the assignment of  $J^f=1^+$  for that state and to a total width of  $\sim 200$  keV, also in good agreement with the present work. Since this is the only  $1^+$  state positively identified in  $^{14}\text{C}$ , it is of special theoretical interest and will be discussed in the section on comparisons to theory calculations.

For  $E_n \gtrsim 3$  MeV the scattering data reveal the growth of large  $B_2$  and  $B_4$  coefficients which dominate the interaction at these energies. For elastic scattering the clear presence of a resonant  $B_4$  term requires  $l_n=2$ . The  $\frac{1}{2}^-$  ground state of  $^{13}\text{C}$  can be described in its most simple configuration as a  $1p_{1/2}$  neutron coupled to a closed  $^{12}\text{C}$  core. Therefore, in the present experiment it is expected that the most probable negative parity state would be a neutron in the  $s$ - $d$  shell coupled to the  $1p_{1/2}$  neutron of the target to give states of  $J^f=0^-, 1^-, 2^-,$  and  $3^-$ . The broad structure in Figs. 1 and 3 between  $E_n=3.2$  and 4.2 MeV is dominated by very broad negative parity states formed primarily by  $d_{3/2}$  and  $d_{5/2}$  neutrons leading to states of possible  $J^f=1^-, 2^-,$  and  $3^-$ . Exhaustive searches for

best fits to the  $B_L$  over the broad structure were made beginning with different initial assumptions in order to converge as nearly as possible to a unique set of resonances and  $R_{cc}^{J^f}$  parameters to describe this group of states. In all cases the best fits converged on the following set of three states: a very broad  $1^-$  state formed almost entirely by the  $d_{3/2}$  channel near  $E_n=3.5$  MeV; a broad  $2^-$  state formed mostly via the  $d_{3/2}$  channel ( $\gamma_{d_{3/2}^2}/\gamma_{d_{5/2}^2}$  of 2.5 to 3) near  $E_n=3.7$  MeV; and a narrower  $1^-$  state near 4.3 MeV formed with roughly comparable amplitudes of  $\gamma_{s_{1/2}}$  and  $\gamma_{d_{3/2}}$ . While the earlier  $\sigma_T$  measurements<sup>1,7</sup> showed a broad resonancelike structure at these energies no previous analysis or assignments were reported for the broader states of this region.

For the resonance at  $E_n=4.77$  MeV and the very broad structure at  $E_n \sim 6.3$  MeV, all three inelastic channels are open. That these groups begin to contribute substantially at this energy is apparent from the increased percentage difference between  $\sigma_T$  and  $\sigma_{el}$  above  $E_n \approx 4.5$  MeV in Fig. 3. Thus from here upward in energy the accuracy of the approximation  $\sigma_T = \sigma_{el}$  becomes less valid. Nevertheless, it is worthwhile to attempt to limit the  $J^f$  and parameters for the resonance and broad structure. From the facts that  $B_4$  is resonant, and that  $B_L$  for  $L > 4$  were negligible, the  $J^f$  for the resonance at  $E_n=4.77$  MeV should be  $1^-, 2^-,$  or  $3^-$ , formed predominantly via the channels of  $d_{3/2}$  and/or  $d_{5/2}$  neutrons. The  $1^-$  assignment clearly disagreed with  $B_4$ . For  $J^f=2^-$  or  $3^-$  the fit was better to all  $B_L$ , but neither allowed a unique assignment. The  $3^-$  assignment gave a slightly better fit, and parameters for this preferred assignment as indicated in Table I were employed in the  $R$ -matrix calculations of Figs. 1 and 3–6. Further evidence to support a preferred  $3^-$  assignment for this state comes from very recent measurements of differential inelastic scattering cross sections for  $^{13}\text{C}(n, n')^{13}\text{C}^*$  (3.09 MeV) made at this laboratory<sup>12</sup> for energies across this resonance. While both the total cross section and integrated elastic cross section showed a resonance, the integrated first inelastic  $^{13}\text{C}(n, n')^{13}\text{C}^*$  (3.09 MeV) cross section did not show any resonant behavior whatever, although the angular distributions did change across the resonance. This would be consistent with a  $3^-$  assignment for the state at  $E_x=12.61$  MeV ( $E_n=4.77$  MeV) because the  $3^-$  could not inelastically decay to the  $\frac{1}{2}^+$  first excited state of  $^{13}\text{C}$  except by  $l_n \geq 3$  which is very unlikely at the low energy ( $E_n \sim 1.5$  MeV) of the inelastic neutrons. On the other hand, a  $2^-$  state would be expected to decay much more easily by  $l_n=1$  to the first excited state of  $^{13}\text{C}$ . Further evidence for  $3^-$  comes from the observation of a broad peak in the proton



TABLE I.  $R$ -matrix parameters for the levels in  $^{14}\text{C}$  used in the calculated curves. A channel radius of  $a = 4.5$  fm was taken for all channels. Only diagonal elements of the  $R_{cc}^{\infty J^\pi}$  background matrix were employed in the fit and are listed under each  $J^\pi$  value. All quantities other than  $E_n$  (lab) and  $\Gamma_T$  (lab) are in the center-of-mass system.

$E_x$ (MeV)	$E_n$ (lab) (MeV)	$E_\lambda$ (MeV)	$J^\pi$	$\Gamma_T$ (lab) <sup>a</sup> (MeV)	$s_{1/2}$	$p_{1/2}$	$\gamma_{\lambda c}$ (MeV <sup>1/2</sup> ) $p_{3/2}$	$d_{3/2}$	$d_{5/2}$
6.09		-3.20	1 <sup>-</sup>		0.70			0	
6.90		-2.10	0 <sup>-</sup>		0.70				
9.789	1.736	1.5951	3 <sup>-</sup>	0.015					0.240
9.806	1.754	1.629	1 <sup>-</sup>	0.041	0.13			0	
10.429	2.426	2.2475	3 <sup>(-)</sup> <sup>b</sup>	0.010					0.123
10.447	2.445	2.270	(1 <sup>+</sup> , 2 <sup>±</sup> ) <sup>c</sup>	0.007		0.059	0		
10.502	2.504	2.3247	$\geq 1$	$\ll 0.005$					
11.29	3.35	3.11	1 <sup>+</sup>	$\approx 0.18$		0.196	0.240		
11.395	3.466	3.219	$\geq 2$	$\leq 0.007$					
11.44	3.51	3.25	1 <sup>-</sup>	( $\sim 1$ ) <sup>d</sup>	0.20			0.90	
11.62	3.71	3.47	2 <sup>-</sup>	( $\sim 0.9$ ) <sup>d</sup>				0.75	0.45
12.22	4.35	4.05	1 <sup>-</sup>	( $\sim 0.5$ ) <sup>d</sup>	0.35			0.25	
12.61	4.77	4.44	(3, 2) <sup>-e</sup>	0.13					0.21
12.867	5.050 <sup>f</sup>								
12.970	5.162 <sup>f</sup>								
13.6	5.9	5.7	(1, 2) <sup>-g</sup>	$\sim 1.3$	0.2			0.9	
			0 <sup>-</sup> $R_{cc}^{\infty}$		-0.15				
			$b_c$		0				
			0 <sup>+</sup> $R_{cc}^{\infty}$			0.25			
			$b_c$			-0.25			
			1 <sup>-</sup> $R_{cc}^{\infty}$		-0.15			0.55	
			$b_c$		0			-1.0	
			1 <sup>+</sup> $R_{cc}^{\infty}$			0.25	0.55		
			$b_c$			-0.25	-0.25		
			2 <sup>-</sup> $R_{cc}^{\infty}$					0.55	0.05
			$b_c$					-1.0	-1.0
			2 <sup>+</sup> $R_{cc}^{\infty}$				0.55		
			$b_c$				-0.25		
			3 <sup>-</sup> $R_{cc}^{\infty}$						0.05
			$b_c$						-1.0

<sup>a</sup>Total neutron width from data of Ref. 7.

<sup>b</sup>For  $J^\pi = 3^+$ ,  $\gamma_{l=3} = 0.37$ .

<sup>c</sup>Curves and parameters are for  $J^\pi = 1^+$ . The  $\gamma_{l=3/2}$  was set equal to zero for convenience only.

<sup>d</sup>Estimation of  $\Gamma_{\lambda n_0}$  from  $\sum_c 2P_c \gamma_{\lambda c}^2$ .

<sup>e</sup>Curves and parameters are for  $J^\pi = 3^-$ .

<sup>f</sup>Observed in Ref. 7 but not included in  $R$ -matrix fit.

<sup>g</sup>Curves and parameters are for  $J^\pi = 1^-$ .

spectrum for the  $^{12}\text{C}(t,p)^{14}\text{C}$  reaction from which the authors<sup>5</sup> make an assignment of  $(2^+, 3^-)$  to a state at  $E_x = 12.58$  MeV in  $^{14}\text{C}$ . Considering the relatively large width of this state observed in that measurement and the locations of other observed states in the region, it is likely that the  $^{12}\text{C}(t,p)^{14}\text{C}$  experiment and the present experiment are dealing with the same state. Since the present experiment rules out positive parity, then the  $^{12}\text{C}(t,p)^{14}\text{C}$  work gives further evidence in favor of the preferred  $3^-$  assignment for this state. It is concluded that  $3^-$  is the probable assignment for the state at  $E_x = 12.61$  MeV although  $2^-$  cannot yet be ruled out.

On the assumption of a single state for the very broad structure above  $E_n = 5.5$  MeV, a resonant  $B_4$  requires a large  $d$ -wave component, or  $J^\pi = 1^-, 2^-,$  or  $3^-$  for the state. For  $J^\pi = 3^-$  the fit strongly disagreed with  $B_3$  and  $B_4$  in the 3 to 4 MeV region. For  $1^-$  and  $2^-$  the fits were much better but in neither case could all  $B_L$  be fitted well, simultaneously. Therefore, it was concluded from this work that  $J^\pi = 1^-$  or  $2^-$  for the assumed single state at  $E_n \approx 5.9$  MeV ( $E_x \approx 13.6$  MeV).

In summary of the experimental results and analysis, the calculated curves shown in all the figures represent the best fits to all the data for  $\sigma_T$  and  $\sigma_{\text{el}}(\theta)$  from just above the neutron separation energy to  $E_n \approx 6.5$  MeV ( $E_x = 14.2$  MeV) and are based on the single set of  $R$ -matrix parameters given in Table I. These results together with other well established states in  $^{14}\text{C}$  are summarized in the level diagram of Fig. 2. This is the first time differential neutron data have been reported for  $^{13}\text{C} + n$ . The analysis of the neutron data far into the unbound region of  $^{14}\text{C}$  has led to a considerable amount of new information concerning this nucleus.

#### D. Comparison with $T=1$ states in $^{14}\text{N}$

Of the very few states in  $^{14}\text{N}$  that have been clearly identified as  $T=1$  in this region of excitation,<sup>6</sup> the  $1^+$  state at  $E_x = 13.71$  MeV seems to be the one most clearly established. Its width and energy (11.34 MeV in  $^{14}\text{C}$ ) are in good agreement with those of the  $1^+$  state in  $^{14}\text{C}$  at 11.29 MeV, so these states are assigned as analogs. A very broad resonance ( $\Gamma \sim 1$  MeV) is reported in the  $^{13}\text{C}(p,\gamma_0)^{14}\text{N}$  reaction at 13.3 MeV in  $^{14}\text{N}$ . It is assigned  $(2^-)$ ,  $T=1$ , and described as part of the giant dipole resonance. The only likely observed candidate for an analog to this state would seem to be the broad  $2^-$  state in  $^{14}\text{C}$  near 11.7 MeV. However, this state in  $^{14}\text{C}$  is clearly several hundred keV above the  $1^+$  state, whereas the broad  $(2^-)$ ,  $T=1$  state in  $^{14}\text{N}$  is centered some 400 keV below the rather clearly established  $1^+$  analog state in

$^{14}\text{N}$ . There is some evidence<sup>6</sup> of inverted ordering of analog states of  $^{14}\text{C}$  and  $^{14}\text{N}$  at lower energies, so perhaps these two may be analogs. Ajzenberg-Selove<sup>6</sup> lists in Table 14.11 of that work two states in  $^{14}\text{N}$  at  $E_x = 11.24$  MeV, one a narrow ( $\Gamma \sim 20$  keV) state of  $J^\pi = (3^-)$  and another much broader one ( $\Gamma = 220$  keV) listed only as  $T=1$ . The nearest known states in  $^{14}\text{C}$  that might reasonably be considered as analogs would be the  $1^-$  and the narrow  $3^-$  states, both of which do fall at essentially the same energy of  $E_x \approx 9.8$  MeV ( $E_n \approx 1.75$  MeV). However, the corresponding energy of these states in  $^{14}\text{N}$  is 12.16 MeV, or nearly 1 MeV higher than the location of the two resonances observed in  $^{14}\text{N}$ . This is comparable with the shift between the possible  $2^-$  analogs discussed above. There is not sufficient identification of  $J^\pi$  and  $T$  for states at these energies in  $^{14}\text{N}$ , to date, to establish firmly enough analog comparisons to show whether or not such large shifts do, in fact, occur.

## IV. MODEL CALCULATIONS

### A. Background

#### 1. Positive parity states

Several calculations have been performed to interpret the level structure of the  $A=14$  nuclei. Most of these calculations have focused on  $^{14}\text{N}$  because of the availability of data for that nucleus. Some of these calculations<sup>13-19</sup> for the positive parity states use shell model configurations  $(1s)^4(1p)^{A-4}$  but some<sup>13,16,17</sup> do not include excitation energies applicable to the present experiment or do not furnish spectroscopic data.<sup>14</sup> Other calculations have described the positive parity states in terms of  $(sd)^2$  configurations coupled to the ground state<sup>20,21</sup> of  $^{12}\text{C}$  and the  $2^+$  first excited state.<sup>22</sup> The states described by these latter calculations are not likely to be seen in neutron elastic scattering from  $^{13}\text{C}$ . There is, however, a singular positive parity state which is clearly identified in the present experiment at  $E_x = 11.29$  MeV with  $J^\pi = 1^+$ . To date this has been the only  $1^+$  state observed in  $^{14}\text{C}$  and is rather pure  $(p_{3/2}^7 p_{1/2}^3)_{1^+}$ , or in an  $^{16}\text{O}$  basis,  $(p_{1/2}^{-1} p_{3/2}^{-1})_{1^+}$ , as indicated by the  $^{15}\text{N}(d, ^3\text{He})^{14}\text{C}$  work of Kaschl *et al.*<sup>2</sup> Thus for a  $^{13}\text{C}_{\text{e.s.}}$  with  $p_{3/2}^7 p_{1/2}^2$  and  $p_{3/2}^6 p_{1/2}^3$  components, the  $1^+$  state in  $^{14}\text{C}$  can be formed simply by adding either a  $p_{1/2}$  or  $p_{3/2}$  neutron.

Cohen and Kurath<sup>15</sup> have calculated spectroscopic factors for stripping leading to positive parity  $T=1$  states in  $A=14$  nuclei. For a  $1^+$ ,  $T=1$  state corresponding to an excitation energy of 9.41 MeV in  $^{14}\text{C}$ , they give spectroscopic factors of  $\sim 10^{-3}$  for transfer of a  $1p_{3/2}$  nucleon and  $\sim 10^{-4}$  for that of a  $1p_{1/2}$  nucleon which would yield  $\theta_{\text{e.c.}}^2$  of the same

magnitude (as discussed later). The  $\theta_{\text{sc}}^2$  derived from Table I is 0.017 for the  $p_{3/2}$  and 0.12 for the  $p_{1/2}$  neutron transfer, that is, several orders of magnitude greater than the predicted values.

Richter and de Kock<sup>19</sup> used the wave functions obtained by Saayman *et al.*<sup>18</sup> in a modified surface delta interaction (MSDI) global calculation for nuclei with  $10 \leq A \leq 14$  to calculate one-particle spectroscopic factors for these nuclei. The calculated spectroscopic factors for the only  $T=1$  unbound state in  $A=14$ , i.e., the  $1^+$  state at 10.59 MeV in  $^{14}\text{N}$  (8.22 MeV in  $^{14}\text{C}$ ), are of the order of  $10^{-3}$ . Thus the calculations of both Cohen and Kurath<sup>15</sup> and Saayman *et al.*<sup>18</sup> severely underestimate the widths of this state as observed in this and other experiments.<sup>2,4</sup> A separate fit by Saayman *et al.* to  $A=14$  nuclei only, which does include the  $1^+$  levels at 3.95 and 13.75 MeV as well as two other  $2^+$  levels, yields, as expected, a better overall fit for  $^{14}\text{N}$ . The result is a  $1^+$  level at an excitation equivalent to 10.84 MeV in  $^{14}\text{C}$ . However, the spectroscopic factor and hence the width is not affected because the  $1^+$  state has only one component.

Small admixtures of  $sd$  orbitals in the wavefunctions of  $^{13}\text{C}$  and  $^{14}\text{C}$  may remedy this situation. Such admixtures are also implied by the rather poor results for the calculated  $M1$  radiative widths<sup>18</sup> of the excited states in  $^{13}\text{C}$  and the calculated  $M1$  ( $1^+ \rightarrow 0^+$ ) transition strength in  $^{14}\text{C}$  which is twice the experimental value.<sup>23</sup> A weak coupling calculation by Lie<sup>10</sup> for the  $A=14$  system using an  $^{16}\text{O}$  core with  $p$  holes and  $sd$  particles yields a  $1^+$ ,  $T=1$  state at an excitation energy of 9.68 MeV in  $^{14}\text{C}$ . This state is a 99% pure ( $p_{1/2}^{-1}p_{3/2}^{-1}$ ) configuration. However, detailed spectroscopic data are not available for this state to check the effect of the addition of  $sd$  nucleons.

## 2. Negative parity states

Shell model calculations for the negative parity states in  $A=14$ , focusing on  $^{14}\text{N}$ , have been carried out by several authors.<sup>10,15,19,20,24-27</sup> Most of the calculations emphasize energies below those of the present experiment. The calculations of Sebe<sup>24</sup> and of Richter and de Kock<sup>19</sup> consider only energies corresponding to the bound states in  $^{14}\text{C}$ . The calculation of True<sup>20</sup> predicts two unbound negative parity states, while the calculations of Cooper and Eisenberg<sup>25</sup> and Hsieh and Horie<sup>26</sup> show three such states. The calculations of Jäger *et al.*<sup>27</sup> and those of Lie<sup>10</sup> extend to higher energies and predict several unbound states as well as reduced widths.

### B. Present calculations

The spectrum of negative parity states of  $^{14}\text{C}$  for excitation energies covered in the present experi-

ment has been calculated by the authors using a core-coupling model, and by Millener and Darema-Rogers<sup>28</sup> using effective interactions. Millener and Darema-Rogers have used the results of Cohen and Kurath<sup>15</sup> for the  $1p$  shell matrix element and those derived from the particle-hole interaction of Millener and Kurath<sup>29</sup> for the  $p$ - $sd$  matrix elements.

The present core-coupling model includes the  $0^+$  ground state and  $2^+$  first excited state in the  $(A-2)$  core,  $^{12}\text{C}$ . In this scheme complex configurations in the  $p$  shell are treated collectively. The Hamiltonian for the core-coupling calculation is

$$H = H_c + H_n - \xi \sum_{n=1}^2 \vec{j}_n \cdot \vec{J}_c - \eta \sum_{n=1}^2 Q_n \cdot Q_c + V_0 [(1-\alpha) + \alpha \vec{\sigma}_1 \cdot \vec{\sigma}_2] \delta(\vec{r}_1 - \vec{r}_2),$$

where  $H_c$  and  $H_n$  are the Hamiltonians for the core and neutrons;  $J_c$  and  $j_n$  are the angular momentum of the core and neutrons, respectively, with  $Q_c$  and  $Q_n$  the mass quadrupole operators for the core and neutrons. The strength parameters are  $\xi$ ,  $\eta$ , and  $V_0$ , and  $\alpha$ . The wave functions are expressed as

$$|E_{\alpha}IM\rangle = \sum_{\substack{j_1 j_2 \\ J J_c}} \langle (j_1 j_2) J J_c : E_{\alpha} I \rangle | [(j_1 j_2) J ]_{\Lambda} J_c : IM \rangle$$

where the subscript  $A$  denotes antisymmetrization for the two nucleons. The Hamiltonian  $H_c + H_n$  is diagonal in this scheme so that the energy of the core replaces  $H_c$  and is taken from  $^{12}\text{C}$  data, while single particle energies replace  $H_n$ . The reduced matrix element for the core  $\langle 0^+ || Q_c || 2^+ \rangle$  is deduced from the  $2^+ \rightarrow 0^+$  transition in  $^{12}\text{C}$  while the  $\langle 2^+ || Q_c || 2^+ \rangle$  matrix element is determined by the relation between reduced matrix elements using rotational wave functions:

$$\frac{\langle 2^+ || Q_c || 2^+ \rangle}{\langle 0^+ || Q_c || 2^+ \rangle} = \left(\frac{7}{10}\right)^{1/2}.$$

The differences between single particle energies are chosen initially to be approximately those

TABLE II.  $^{14}\text{C}$  parameters [coupling:  $\xi$  (MeV) = -0.330,  $\eta$  (MeV fm<sup>-2</sup>) = 0.210.  $\delta$ :  $V_0$  (MeV) = 100.0,  $\alpha = 0.400$ ].

Single particle		Core	
$j$	$E_j$ (MeV)	$J_c$	$E_c$ (MeV)
$s_{1/2}$	5.700	$0^+$	0
$d_{5/2}$	6.000	$2^+$	4.43
$d_{3/2}$	11.100		

found in  $^{13}\text{C}$  while  $\xi$ ,  $\eta$ ,  $V_0$ , and  $\alpha$  are determined in the fitting. These values are given in Table II.

Spectroscopic factors are easily obtained in the model calculations. These spectroscopic factors have been used to calculate dimensionless reduced widths  $\theta^2$  using the relationship<sup>30</sup>

$$\theta^2 = S\theta_0^2,$$

where  $S$  is the spectroscopic factor and  $\theta_0^2$  is a dimensionless single particle reduced width.

In the core-coupling calculation, spectroscopic factors are obtained from the wave functions by a simple recoupling in which the wave function represents an ( $sd$ ) neutron coupled to the ground state of  $^{13}\text{C}$  taken to be  $[0^+(^{12}\text{C}) \times p_{1/2}]_{1/2}$ . This assumption is reasonable in view of the relatively pure ( $\sim 70\%$ )  $p_{1/2}$  nature<sup>13,31</sup> of the ground state of  $^{13}\text{C}$ . The spectroscopic factors are given by

$$S_{ij} = |\langle (j_1 j_2) J_0 : E_\alpha J \rangle|^2.$$

In the calculation of Millener and Darema-Rogers the spectroscopic factor is simply related to the square of the single particle coefficient of fractional parentage for the appropriate ( $sd$ ) nucleon coupled to  $^{13}\text{C}_{g.s.}$  Lie also calculates spectroscopic factors as simple overlaps. Those values have to be multiplied by a factor of 2 for the  $^{14}\text{C}$  case.

### C. Results and discussion

The calculated spectra and spectroscopic information for the negative parity states from Millener and Darema-Rogers and from the present calculations together with the results of the present experiment are summarized in Table III. Figure 7 presents the above calculated spectra, the spectrum of Lie adjusted to  $^{14}\text{C}$ , and the experimental spectrum. Correspondence between experimental levels and calculated states can be made based on the energies and reduced widths given in Table III. The calculated  $\theta_{s_{1/2}}^2$  of the core-coupling calculations were normalized to the  $0^-$  experimental level so that  $(\theta_0^2)_{s_{1/2}} = 0.176$ . This value was used also for the computation of  $\theta_{s_{1/2}}^2$  derived from the calculations of Millener and Darema-Rogers (MDR). The spectroscopic factors  $S_{s_{1/2}}$  and  $S_{d_{5/2}}$  are large for the bound states in the core-coupling calculation, the effective interaction calculation of MDR, and the calculation of Lie (adjusted to  $^{14}\text{C}$ ). There is, on the whole, relatively good agreement among the spectroscopic factors from these three independent calculations. Additional confidence in these spectroscopic factors comes from the fact that calculated values of  $S_{s_{1/2}}$  and  $S_{d_{5/2}}$  are in good agreement with the values derived from the  $^{13}\text{C}(\bar{d}, p)^{14}\text{C}$  data of Datta *et al.*<sup>32</sup> for the  $1^-$  and  $2^-$

bound states. There is some uncertainty regarding the proper values of  $\theta_0^2$ . Lie<sup>10</sup> and others have found that  $(\theta_0^2)_{d_{3/2}} = (\theta_0^2)_{d_{5/2}} = 0.40$  gave good agreement with data. These values were used to calculate the appropriate  $\theta_{sc}^2$  of Table III from spectroscopic factors for the MDR and core-coupling calculations, and gave reasonable agreement with the neutron data of the present experiment.

It is seen from Fig. 7 that the three calculations reproduce many of the spins and parities of the levels for which these quantities have been assigned. For the bound states, all calculations, as expected, reproduce the spins and parities. Near 10 MeV all calculations show both a  $3^-$  and a  $1^-$  state. The  $3^-$  and  $1^-$  states in all three calculations are identified with both the  $3^-$  and  $1^-$  states observed experimentally by neutrons at 9.79 and 9.81 MeV, respectively. The calculated reduced widths for these states are small in all three calculations, in agreement with experiment.

The experimental spectrum has three closely spaced levels at 10.43, 10.45, and 10.50 MeV. The first of these is assigned  $J^\pi = 3^-(^-)$ , while the next two have possible assignments in this experiment of  $(1^*, 2^+)$  and  $\geq 1$ , respectively. The level at 10.50 MeV also has been suggested<sup>5,21</sup> to be  $3^+$  rather than  $(3^-)$ . Having identified the first two  $3^-$  states in the MDR and core-coupling calculations with the experimentally observed ones at 6.73 and 9.79 MeV, it is reasonable to identify tentatively the third and fourth  $3^-$  states of each calculation with the states at 10.43 and 12.61 MeV, respectively, both of which are tentatively assigned  $3^-$  in this work.

The calculations all yield states which correspond to several levels in the next group of experimental levels above 11 MeV. In this group there are two experimental levels with  $J^\pi = 1^-$ , one at 11.44 MeV, the other at 12.22 MeV. The core-coupling model yields two  $J^\pi = 1^-$  states in this region. The lower of the two, at 10.50 MeV, is somewhat low in energy but yields a value for  $\theta_{d_{3/2}}^2$  in good agreement with the experimental value for the 11.44 MeV level. The calculated reduced widths of the upper  $1^-$  state at 12.24 MeV are in fair agreement with the experimental values for the 12.22 MeV level. The MDR calculation yields one  $1^-$  state in the region, at 12.00 MeV, with  $\theta_{d_{3/2}}^2$  also in good agreement with the experimental value for the 11.44 MeV level. In both these calculations  $\theta_{s_{1/2}}^2 < 10^{-3}$  or smaller for the states corresponding to the experimental level at 11.44 MeV. The calculation of Lie yields a  $1^-$  state at 10.75 MeV in  $^{14}\text{C}$  but this state has no reduced neutron width. Figure 4 of Lie's work shows another  $1^-$  state at approximately 11.7 MeV, but no spectroscopic data are available for this state.

TABLE III. Energy spectrum and dimensionless reduced widths  $\theta_{\lambda c}^2$  for  $^{14}\text{C}$  from the present experiment, the core-coupling calculations, and MDR calculations. Experimental  $\theta_{\lambda c}^2 = (2\mu a^2/3\hbar^2)\gamma_{\lambda c}^2$  are determined from Table I with  $a = 4.5$  fm. Values of  $\theta_{\lambda c}^2 < 10^{-2}$  are not tabulated.

$E_x$ (MeV)	Experimental				Core-coupling calculations					MDR calculations				
	$J^\pi$	$s_{1/2}$	$\theta_{\lambda c}^2$ $d_{3/2}$	$d_{5/2}$	$E_x$ (MeV)	$J^\pi$	$s_{1/2}$	$\theta_{\lambda c}^2$ $d_{3/2}$	$d_{5/2}$	$E_x$ (MeV)	$J^\pi$	$s_{1/2}$	$\theta_{\lambda c}^2$ $d_{3/2}$	$d_{5/2}$
6.09	$1^-$	0.15			6.34	$1^-$	0.15			6.19	$1^-$	0.15	0.01	
6.73	$3^-$				6.76	$3^-$			0.35	6.52	$3^-$			0.38
6.90	$0^-$	0.15			7.08	$0^-$	0.15		0.35	7.44	$2^-$		0.04	0.24
7.34	$2^-$				7.67	$2^-$			0.33	7.60	$0^-$	0.20		
					9.62	$2^-$			0.02					
9.79	$3^-$			0.02										
9.81	$1^-$	0.01			9.84	$3^-$			0.02					
					10.18	$1^-$	0.01	0.03						
										10.36	$3^-$			
10.43	$3^{(-)}$													
10.45	$(1^+, 2^+)$													
10.50	$>1$				10.50	$1^-$		0.20						
										10.55	$2^-$		0.16	0.13
										10.58	$1^-$	0.03		
					10.87	$2^-$		0.01						
11.29	$1^+$				11.32	$4^-$								
11.40	$\geq 2$													
11.44	$1^-$	0.01	0.25		11.48	$2^-$		0.12						
										11.51	$2^-$		0.11	
11.62	$2^-$		0.17	0.06	11.77	$3^-$								
										12.00	$1^-$		0.24	
										12.13	$4^-$			
12.22	$1^-$	0.04	0.02		12.24	$1^-$	0.02	0.04						
12.61	$(3, 2)^-$			0.01										
12.87	$(2^+, 3^-)^a$													
	$(4, 5)^b$													
12.96	$(1^-)^a$													
	$(3, 4)^b$													
					13.41	$2^-$		0.02	0.06	13.11	$3^-$			
					13.43	$0^-$	0.02							
										13.44	$2^-$		0.11	0.03
										13.50	$4^-$			
					13.61	$1^-$		0.08						
					13.65	$3^-$			0.03					
13.6	$(1, 2)^-$	0.01	0.25											
					14.30	$2^-$		0.13		14.30	$5^-, 1^-$			
										14.43	$3^-$			0.03
										14.53	$0^-$			
	Many levels, no assignments				14.58	$5^-$								
										14.87	$2^-$			

<sup>a</sup>Tentative assignments from Ref. 5.

<sup>b</sup>Tentative assignments from Ref. 3.

The calculation of MDR yields two  $2^-$  states in the unbound region below 12.5 MeV, while the core-coupling model yields three. Only one  $2^-$  level is currently identified experimentally. In the case of the core-coupling calculation the lowest

two of these three  $2^-$  states essentially are core excited states with negligible neutron widths. Thus the  $2^-$  state at 11.48 MeV is taken to correspond to the experimental  $2^-$  level at 11.62 MeV. In the MDR calculation the corresponding state is at

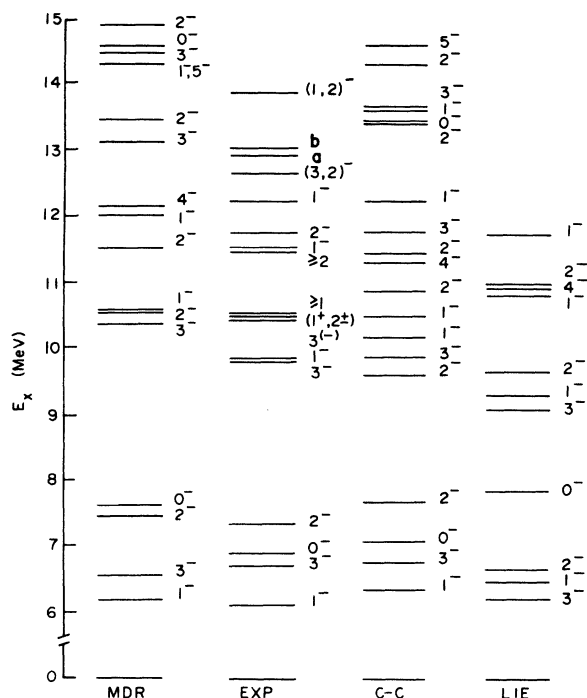


FIG. 7. Experimental and calculated levels for  $^{14}\text{C}$  condensed from Table III together with the results of Ref. 10. References to states labeled "a" (12.87 MeV) and "b" (12.96 MeV) are given in Table III.

10.55 MeV and has reduced widths in good agreement with the experimental values. The calculation of Lie yields two  $2^-$  states in this region: one at 9.62 MeV, the other at 10.94 MeV with  $\theta_{d_{3/2}^2} = \theta_{d_{5/2}^2} = 0.07$  for the lower level, and  $\theta_{a_{3/2}^2} = 0.07$

for the upper level.

All three models predict a  $4^-$  state below 12.5 MeV which has not been observed. The MDR and core-coupling calculations also predict a  $5^-$  state above 14 MeV. Experimentally Mordechai *et al.*<sup>5</sup> have observed a level at 11.67 MeV which they have assigned tentatively as  $5^-$ , while Ajzenberg-Selove *et al.*<sup>3</sup> have tentatively assigned  $5^-$  to the level observed at 11.72 MeV. Other correspondence between experimental levels and calculated states above 12.50 MeV will have to await resolution of the uncertainties in the experimental assignments for that region.

The present experiment yields much new information on the structure of the  $^{14}\text{C}$  nucleus, while calculations show that the spectrum of negative parity states can be interpreted with a considerable degree of success in terms of simple models.

#### ACKNOWLEDGMENTS

The authors are particularly indebted to J. Milner and F. Darema-Rogers for providing to us prior to publication the very interesting results of their shell-model calculations on  $^{14}\text{C}$  for use in this work. Their helpful cooperation clearly added substantially to the value of this effort. The authors also thank David Resler and Paul Koehler for invaluable assistance in both the experiment and data analysis. Special thanks are given to David Sturbois and Donald Carter of the accelerator staff without whose dedicated extra efforts much of the results reported here might never have been achieved. This work was supported by the U. S. Department of Energy.

<sup>1</sup>H. Cohn, J. K. Bair, and H. B. Willard, *Phys. Rev.* **122**, 534 (1961).

<sup>2</sup>G. Kaschl, G. Mairle, H. Mackh, D. Hartwig, and U. Schwinn, *Nucl. Phys.* **A178**, 275 (1971).

<sup>3</sup>F. Ajzenberg-Selove, H. G. Bingham, and J. D. Garrett, *Nucl. Phys.* **A202**, 152 (1973).

<sup>4</sup>H. Crannell, J. M. Finn, P. Hallowell, J. T. O'Brien, N. Ensslin, L. W. Fagg, E. C. Jones, Jr., and W. L. Bendel, *Nucl. Phys.* **A278**, 253 (1977).

<sup>5</sup>S. Mordechai, H. T. Fortune, G. E. Moore, M. E. Coburn, R. V. Kollarits, and R. Middleton, *J. Phys. G* **4**, 407 (1978); *Nucl. Phys.* **A301**, 463 (1978).

<sup>6</sup>F. Ajzenberg-Selove, *Nucl. Phys.* **A268**, 1 (1976).

<sup>7</sup>G. F. Auchampaugh, S. Plattard, and N. W. Hill, *Nucl. Sci. Eng.* **69**, 30 (1979).

<sup>8</sup>R. M. White, R. O. Lane, H. D. Knox, and J. M. Cox, *Nucl. Phys.* **A340**, 13 (1980).

<sup>9</sup>R. N. Glover and A. D. W. Jones, *Nucl. Phys.* **84**, 673 (1966).

<sup>10</sup>S. Lie, *Nucl. Phys.* **A181**, 517 (1972).

<sup>11</sup>P. E. Koehler, D. A. Resler, H. D. Knox, R. M.

White, and R. O. Lane, *Bull. Am. Phys. Soc.* **24**, 656 (1979).

<sup>12</sup>D. Resler, Ohio University Report No. DOE/ER/02490-1, 1980 (unpublished).

<sup>13</sup>E. K. Warburton and W. T. Pinkston, *Phys. Rev.* **118**, 733 (1960).

<sup>14</sup>D. Amit and A. Katz, *Nucl. Phys.* **58**, 388 (1964).

<sup>15</sup>S. Cohen and D. Kurath, *Nucl. Phys.* **A101**, 1 (1967).

<sup>16</sup>E. C. Halbert, Y. E. Kin, and T. T. S. Kuo, *Phys. Lett.* **20**, 657 (1966).

<sup>17</sup>P. Goldhammer, J. R. Hill, and J. Nachamkin, *Nucl. Phys.* **A106**, 62 (1968).

<sup>18</sup>R. Saayman, P. R. deKock, and J. H. Van der Merwe, *Z. Phys.* **265**, 69 (1973).

<sup>19</sup>W. A. Richter (private communication); W. A. Richter and P. R. deKock, *Z. Phys. A* **282**, 207 (1977).

<sup>20</sup>W. W. True, *Phys. Rev.* **130**, 1530 (1963).

<sup>21</sup>H. T. Fortune, M. E. Cobern, S. Mordechai, G. E. Moore, S. Lafrance, and R. Middleton, *Phys. Rev. Lett.* **40**, 1236 (1978).

<sup>22</sup>P. Hoffmann-Pinther and R. O. Lane, *Bull. Am. Phys.*

- Soc. 24, 590 (1979).
- <sup>23</sup>D. Kurath (private communication).
- <sup>24</sup>T. Sebe, Prog. Theor. Phys. 30, 290 (1963).
- <sup>25</sup>B. S. Cooper and J. M. Eisenberg, Nucl. Phys. A114, 184 (1968).
- <sup>26</sup>S. T. Hsieh and H. Horie, Nucl. Phys. A151, 243 (1970).
- <sup>27</sup>H. U. Jäger, H. R. Kissener, and R. A. Eramzhian, Nucl. Phys. A171, 16 (1971).
- <sup>28</sup>D. J. Millener and F. Darema-Rogers (private communication).
- <sup>29</sup>D. J. Millener and D. Kurath, Nucl. Phys. A255, 315 (1975).
- <sup>30</sup>M. H. Macfarlane and J. B. French, Rev. Mod. Phys. 32, 567 (1960).
- <sup>31</sup>F. Darema-Rogers (private communication).
- <sup>32</sup>S. K. Datta, G. P. A. Berg, and P. A. Quin, Nucl. Phys. A312, 1 (1978).